A Rotordynamic Analysis of Circumferentially-Grooved Pump Seals Based on a Three-Control-Volume Theory

Tae Woong Ha*

Mechanical Design & Production Engineering Department, Kyung-won University

An Sung Lee

Rotor Dynamics Group, Korea Institute of Machinery and Materials

In this paper the leakage prediction and rotordynamic analysis of an annular seal with a smooth rotor and circumferentially grooved stator are performed based on a three-control-volume theory. The present analysis is validated by comparing with the experimental data of Iwatsubo and Sheng and theoretical results suggested by Marquette and Childs. For the leakage prediction the present analysis shows a good agreement with Marquette and Childs' result and a qualitation agreement with Iwatsubo and Shengs' experimental data. Direct and cross-coupled stiffness coefficients show closer agreement with the experimental values than those of Marquette and Childs. However, direct damping coefficient shows greater discrepancy from the experimental value than Marquette and Childs'.

Key Words : Rotordynamic Analysis, Grooved pump seal, Control-Volume Analysis, Friction-Factor Model, Leakage, Rotordynamic Coefficients

Nomenclature

B	: Depth of groove
C, c	: Direct and cross-coupled damping coefficients (N · s/m)
C_r	: Grooved seal clearance (mm)
f	: Frequency ratio (Ω/ω) in Eq. (17)
f_s, f_r	: Fanning friction factors of stator and rotor surface
F_X, F_Y	: Components of seal reaction force in X-Y coordinate system (N)
F_r, F_θ	: Components of seal reaction force in r-θ coordinate system (N)
H	: Local seal clearance (mm)
K, k	: Direct and cross-coupled stiffness coefficients (N/m)
L	: Seal length (mm)
M, m	: Added mass and cross-coupled

	added mass coefficients (N · s²/m)
P	: Pressure (bar)
P_R, P_s	: Seal entrance pressure and exit pressure (bar)
R	: Radius of rotor (mm)
t	: Time (s)
U	: Fluid velocity in the circumferential direction (m/s)
U_s, U_r	: Bulk-flow velocities relative to stator and rotor of Eq. (4)
V	: Radial velocity of the flow at the interface between control volume Ⅱ and Ⅲ
W	: Fluid velocity in the axial direction (m/s)
W_0	: Average axial fluid velocity in a land part (m/s)
x, y	: Rotor displacements from its static position (m)
Z	: Axial coordinate
α	: Groove penetration angle (rad)
ε	: Eccentricity ratio
ρ	: Fluid density (kg/m³)
θ	: Angular coordinate

* Corresponding Author,
  E-mail : TWHA@Mail. Kyungwon. ac. kr
  TEL : +82-342-750-5308 ; **FAX** : +82-342-750-5273
  Mechanical Design & Production Engineering Department, Kyung-won University, San 61 Bokjung-dong Soojung-gu, Sungnam, Kyunggi-do 461-702, Korea.

ω : Rotor angular velocity (rad/s)

Subscripts

Ⅰ , Ⅱ , Ⅲ : Relative to control volume Ⅰ , Ⅱ , or Ⅲ

0, 1   : Zeroth and first-order perturbations

g   : Groove part

ℓ : Land part

s, r   : Stator, rotor

1. Introduction

Circumferentially grooved seals are widely used in high-performance turbomachinery due to their good leakage property. The current trends of turbomachinery design stress more compact and higher power machines with greater efficiencies. These trends entail higher rotor speeds and tighter clearances, and necessitate more accurate determination of rotor critical speeds, vibration levels, and the onset of instability. The calculations require knowledge of the forces acting on the rotor from seals during machine operation.

The objective of this analysis is to predict leakage and rotordynamic forces developed in annular pressure seals with circumferential grooves subjected to incompressible turbulent flow. The fluid forces acting on the rotor inside a grooved seal are represented by the linearized equation of motion for small amplitude rotor whirl(Eq. (1)). The analysis to be developed in this paper will defines the rotordynamic coefficients for annular seals with smooth rotors and circumferentially grooved stators.

$$-\begin{Bmatrix} F_x \\ F_y \end{Bmatrix} = \begin{bmatrix} K & k \\ -k & K \end{bmatrix} \begin{Bmatrix} x \\ y \end{Bmatrix} + \begin{bmatrix} C & c \\ -c & C \end{bmatrix} \begin{Bmatrix} \dot{x} \\ \dot{y} \end{Bmatrix} + \begin{bmatrix} M & m \\ -m & M \end{bmatrix} \begin{Bmatrix} \ddot{x} \\ \ddot{y} \end{Bmatrix} \qquad (1)$$

Since Black and Cochran(1973) firstly published the analysis of serrated liquid seals, many theories and experiments have been developed for obtaining leakage and rotordynamic coefficients of circumferentially grooved liquid seals(Childs and Kim(1986), Nordmann et al. (1986), Kim and Childs(1987), Iwatsubo and Sheng(1990),

Iwatsubo et al. (1990), Kilgore and Childs (1990), Florjancic(1990), and Marquette and Childs(1996)). Iwatsubo and Cheng(1990) developed a two-control-volume analysis by setting up control volumes in both the land part and groove part. Their analysis showed good qualitative agreement with experiments. Florjancic (1990) developed a three-control-volume theory by defining geometrical two control volumes in the groove part that yielded good predictions for leakage as well as rotordynamic coefficients. Recently, Marquette and Childs(1996) improved on the Florjancic's three-control-volume analysis by setting two control volumes as flow stream line in the groove part and were able to obtain reasonable and consistent results.

In this work, leakage prediction and rotordynamic analysis of an annular seal using a smooth rotor and circumferentially grooved stator is developed based on the three-control-volume theory. The present analysis is validated by comparing with the experimental data of Iwatsubo and Sheng(1990) and theoretical results of Marquette and Childs(1996).

2. Mathematical Modeling

Figures 1 and 2 show the geometry of circumferentially grooved seal and the three-control-volume defined for the present analysis, respectively. The fluid flow in the grooved seal is developed by a pressure difference between the entrance and exit of the seal and rotation of the rotor. The flow passes through the land part and groove part in succession. In the groove part, the flow is divided into through-flow section and
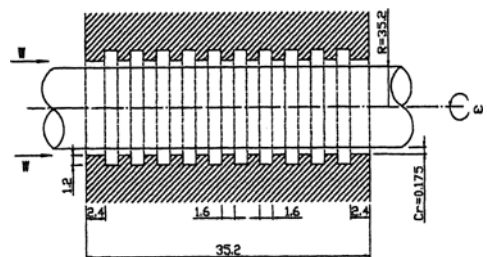

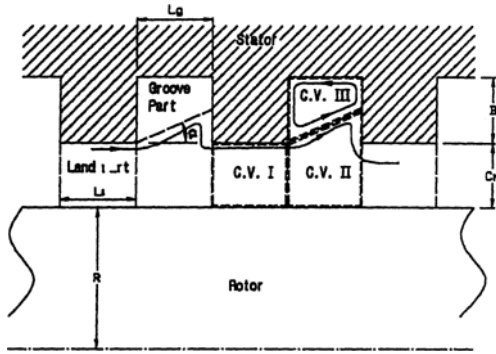**Fig. 1** Geometry of circumferentially grooved seal (Unit : mm)

Fig. 2 Definition of three-control volume for grooved seal

groove cavity with a diverging stream line due to the sudden expansion of the cross-sectional area. Control volume Ⅰ is located in the land part. Control volumes Ⅱ and Ⅲ are located in the groove part, and their boundary coincide with the diverging stream line which is assumed to be straight line of slope α.

For a fully developed turbulent flow regime, assumptions for the present analysis are as follows:

(1) The fluid is Newtonian and incompressible

(2) Shear stress variation for each control volume is ignored and only shear stresses at the boundaries of the control volume are taken into account.

(3) There is no zeroth-order mass exchange between control volumes Ⅱ and Ⅲ.

(4) The pressure variation in the groove is ignored.

(5) A single-vortex flow stays within the groove cavity (control volume Ⅲ).

2.1 Governing equation of control volume Ⅰ

Governing equation of control volume Ⅰ in land part is the same as that of annular smooth seal case. Based on Hirs'(1973) bulk-flow approach and Blasius' surface friction factor model, three equations of continuity, axial-momentum, and circumferential momentum are derived (Ha(1998)) as shown in Eqs. (2)–(4).

Continuity:

$$\frac{\partial H_I}{\partial t} + \frac{\partial}{\partial Z}(W_I H_I) + \frac{1}{R}\frac{\partial}{\partial \theta}(U_I H_I) = 0 \quad (2)$$

Axial-momentum:

$$-H_I\frac{\partial P_I}{\partial Z} = \frac{\rho}{2}f_{sI}W_I U_{Is} + \frac{\rho}{2}f_{rI}W_I U_{Ir}$$
$$+ \rho H_I\left\{\frac{\partial}{\partial t}(W_I) + W_I\frac{\partial}{\partial Z}(W_I) + \frac{U_I}{R}\frac{\partial}{\partial \theta}(W_I)\right\} \quad (3)$$

Circumferential momentum:

$$-\frac{H_I}{R}\frac{\partial P}{\partial \theta} = \frac{\rho}{2}U_I U_{sI}f_{sI} + \frac{\rho}{2}(U_I - R\omega)$$
$$U_{Ir}f_{rI} + \rho H_I\left\{\frac{\partial}{\partial t}(U_I) + \frac{U_I}{R}\frac{\partial U_I}{\partial \theta} + W_I\frac{U_I}{\partial Z}\right\} \quad (4)$$

$$U_{Is} = (W_I^2 + U_I^2)^{\frac{1}{2}}$$

$$U_{Ir} = (W_I^2 + (U_I - R\omega)^2)^{\frac{1}{2}}$$

$$f_{sI} = n_s\left(\frac{2\rho H_I U_{Is}}{\mu}\right)^{m_s}$$

$$f_{rI} = n_r\left(\frac{2\rho H_I U_{Ir}}{\mu}\right)^{m_r}$$

2.2 Governing equation in control volume Ⅱ

Figure 3 shows a coordinate system defined in control volumes Ⅱ and Ⅲ for the theoretical analysis. Three governing equations in control volume Ⅱ are given in Eqs. (5)–(7).

Continuity:

$$\frac{\partial H_{II}}{\partial t} + \frac{\partial}{\partial Z}(W_{II}H_{II}) + \frac{1}{R}\frac{\partial}{\partial \theta}(U_{II}H_{II})$$
$$+ V = 0 \quad (5)$$

Axial-momentum:

$$-H_{II}\frac{\partial P_{II}}{\partial Z} = \frac{\rho}{2}f_{rII}W_{II}U_{IIr} + 1.88\,\rho\,\beta_z^2|\,V_{II}$$
$$- V_{III}|(W_{II} - \overline{W_{III}}) + \rho H_{II}\left\{\frac{\partial}{\partial t}(W_{II})\right.$$
$$\left. + W_{II}\frac{\partial}{\partial Z}(W_{II}) + \frac{U_{II}}{R}\frac{\partial}{\partial \theta}(W_{II})\right\}$$
$$+ \rho V(W_j - W_{II}) \quad (6)$$

Circumferential momentum:

$$-\frac{H_{II}}{R}\frac{\partial P_{II}}{\partial \theta} = \frac{\rho}{2}f_{rII}(U_{II} - R\omega)\,U_{IIr} + 1.88$$
$$\rho\,\beta_s^2|\,V_{II} - V_{III}|(U_{II} - \overline{U_{III}})$$
$$+ \rho H_{II}\left\{\frac{\partial}{\partial t}(U_{II}) + W_{II}\frac{\partial}{\partial Z}(U_{II})\right.$$
$$\left. + \frac{U_{II}}{R}\frac{\partial}{\partial \theta}(U_{II})\right\} + \rho V(U_j - U_{II}) \quad (7)$$

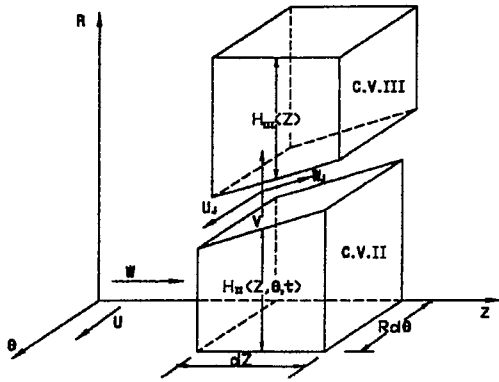$$U_{IIr} = (W_{II}^2 + (U_{II} - R\omega)^2)^{\frac{1}{2}}$$

Fig. 3 Coordinate system in control volumes Ⅱ and Ⅲ

$$f_{rII} = n_r \left(\frac{2\rho H_{II} U_{IIr}}{\mu} \right)^{m_r}$$

U_j and W_j are circumferential and axial velocity components at the boundary of control volumes Ⅱ and Ⅲ, respectively. U_j and W_j can be expressed by the interface jet shear stress definition of Wyssman et al. (1984) as given in Eqs. (8)-(9).

$$W_j = 0.42 \overline{W_{III}} + 0.58 W_{II} \tag{8}$$

$$U_j = 0.42 U_{III} + 0.58 U_{II} \tag{9}$$

Using Prandtl's mixing length hypothesis, the axial and circumferential components of the interface jet shear stresses are given by second terms of right hand side of Eqs. (6)-(7), respectively. β_z and β_θ denote numerical parameters dependint on the groove geometry. In this study, 0.275 is used for β_z and β_θ. $|V_{II} - V_{III}|$ is defined as shown in Eq. (10).

$$|V_{II} - V_{III}|^2 = (U_{II} - U_{III})^2 + (W_{II} - \overline{W_{III}})^2 \tag{10}$$

$\overline{W_{III}}$ is the axial velocity of vortex in the groove cavity and defined by Eq. (11). 0.794 is used for β_v which is dependent on the groove geometry.

$$\overline{W_{III}} = (1 - \beta_v) \overline{W_{II}} \tag{11}$$

2.3 Governing equation of control volume Ⅲ

In control volume Ⅲ, a single-vortex flow is assumed. Therefore, the axial and radial bulk-flow velocities are zero and only circumferential velocity component remains. Two equations are available as given in Eqs. (12)-(13).

$$\frac{H_{III}}{R} \frac{\partial U_{III}}{\partial \theta} - V = 0 \tag{12}$$

$$-\frac{H_{III}}{R} \frac{\partial P_{II}}{\partial \theta} = -1.88 \rho \, \beta_\theta^2 |V_{II} - V_{III}| (U_{II}$$
$$- U_{III}) + \frac{\rho}{2} f_{IIIs} U_{III} U_{IIIs} - \frac{\partial}{\partial z} (H_{III} \, \tau_{gw\theta})$$
$$+ \rho H_{III} \left(\frac{\partial U_{III}}{\partial t} + \frac{U_{III}}{R} \frac{\partial}{\partial \theta} (U_{III}) \right)$$
$$+ \rho V (U_{III} - U_j) \tag{13}$$

$$U_{IIIs} = (U_{III}^2 + (\overline{W_{III}})^2)^{\frac{1}{2}}$$

$$f_{sIII} = n_r \left(\frac{2\rho H_{III} U_{IIIs}}{\mu} \right) m_r$$

where $\tau_{gw\theta}$ denotes the circumferential component of shear stress due to groove walls and is assumed to be linearly distributed between the two groove walls.

3. Solution Procedure

The governing Eqs. (2)-(13) can be nondimensionalized by using nondimensional parameters as defined in Eq. (14). Only the definition of nondimensionalized time is different from those of Marquette and Childs' (1996).

$$w = \frac{W}{W_o}, \quad u = \frac{U}{R\omega}, \quad p = \frac{P}{\rho W_o^2}, \quad h_{I,II} = \frac{H}{C_r},$$
$$z = \frac{Z}{L}, \quad T = \frac{L}{W_o}, \quad \tau = \omega t, \quad b = \frac{R\omega}{W_o},$$
$$u_s = \frac{U_s}{W_o}, \quad u_r = \frac{U_r}{W_o}, \quad |v_{II} - v_{III}| = \frac{|V_{II} - V_{III}|}{W_o} \tag{14}$$

Nondimensionalized governing equations, which are slightly different from those of Marquette and Childs(1996) due to different nondimensionalized time, are defined in Appendix A. Assuming small whirling motion of the rotor about its geometric center, the pressure, axial velocity, circumferential velocity, and local clearance can be expanded in terms of zeroth-order and first-order nondimensionalized perturbation variables (Eq. (15)). Substitution of these perturbed variables into the governing equations yields a set of zeroth-order and first-order equations as defined in Appendix B. Several terms are different in the zeroth-order and first-order equations compared with Marquette and Childs' (1996) results because of using a different nondimensionalized time parameter and correcting possible errors during

Fig. 4 Boundary conditions for grooved seal analysis
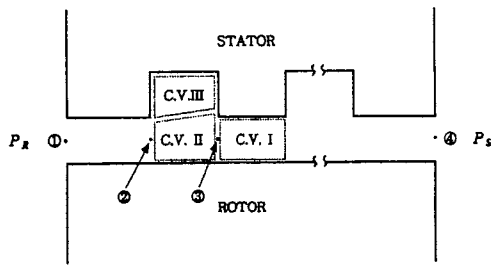
① $P_R - P_I(0) = \dfrac{1+\xi_{in}}{2}\rho\, W_I^2(0)$

② $P_I(L_i) = P_{II}(0)$

③ $P_{II}(L_g) - P_I(0) = \dfrac{1}{2}\left[1 - \left(Cr\,Cr + L_g\tan\alpha\right)^2\right.$

$\left. + \xi_{21}\right]\rho\, W_I^2(0)\,B$

④ $P_s - P_I(L_i) = \dfrac{1+\xi_{ex}}{2}\rho\, W_I^2(L_i)$

the derivation (e.g., M_9 and N_9 in Appendix B).

$$p(z,\ \theta,\ \tau) = p_0(z) + \varepsilon\ p_1(z,\ \theta,\ \tau)$$
$$w(z,\ \theta,\ \tau) = w_0(z) + \varepsilon\ w_1(z,\ \theta,\ \tau) \quad (15)$$
$$u(z,\ \theta,\ \tau) = u_0(z) + \varepsilon\ u_1(z,\ \theta,\ \tau)$$
$$h(z,\ \theta,\ \tau) = h_0(z) + \varepsilon\ h_1(z,\ \theta,\ \tau)$$

The nonlinear zeroth-order equations (see Appendix B) are numerically integrated using Newton-Raphson and Runge-Kutta Methods to yield matched boundary conditions. Figure 4 shows the boundary conditions used in this analysis. ξ_{in} denotes the entrance loss coefficient due to sudden contraction of the cross-sectional area at the seal entrance. ξ_{ex} denotes the pressure recovery factor due to sudden expansion of the cross-sectional area at the seal exit. ξ_{21} denotes the minor loss coefficient due to a change in the cross-sectional area at the interface between control volume Ⅰ and Ⅱ.

In the integration process through the seal, different sets of equations depending on whether the axial position is in the land part (control volume Ⅰ) or the groove part (control volume Ⅱ and Ⅲ) are alternately used since the seal is composed of the interleaving land and groove regions. The solution of the zeroth-order equations yields centered pressure and velocity distributions across the seal. Consequently, leakage

$(\dot{Q})$ through the grooved seal is defined by

$$\dot{Q} = 2\pi R C_r W_0 \quad (16)$$

Along with the results of the zeroth-order solution, the first-order equations (see Appendix B) are solved to calculate hydrodynamic forces developed from the grooved seal. A separation-of-variable solution approach is used for the first-order equations. By assuming a circular precessional motion, the time dependency in the governing equations is eliminated. A transition-matrix approach descibed in Meirovitch (1985), is used to solve the first-order equations. The first-order pressure solution is then integrated axially and circumferentially to determine the rotor-dynamic coefficients. The theoretical hydrodynamic forces are given in terms of the radial and tangential forces. As shown in Eq. (17), the radial and tangential force components can be expressed as a function of f, the ratio of the precession frequency to the rotor speed, by the coordinate transformation of Eq. (1).

$$F_r(f) = -K - fc + f^2 M$$
$$F_\theta(f) = k - fC - f^2 m \quad (17)$$

Briefly, the rotordynamic coefficients are obtained by calculating $F_r(f)$ and $F_\theta(f)$ for a given range of f and then applying the least-squares curve fit on Eq. (17).

4. Results and Analysis Validation

To validate the present analysis Iwatsubo and Sheng's (1990) test grooved seal is applied. The results of the present analysis are compared with Iwatsubo and Shengs' experimental results and Marqutte and Childs' (1996) theoretical results. Only K, k, and C among rotordynamic coefficients are illustrated because M, m, and c are relatively small in value. Figure 1 shows the circumferentially grooved test seal geometry of Iwatsubo and Sheng and the corresponding test conditions are listed in Table 1.

Figure 5 shows the comparison of the leakage results. The result of the present analysis is very close to Marquette and Childs' theoretical result. The theoretical predictions of the present analysis

Table 1 Input data for the analysis of a groove seal

Pressure difference (P_R-P_S)	5.88 (Bar)
Groove length (L_g)	1.6 (mm)
Groove depth (B)	1.2 (mm)
Land part length (L_l)	1.6 (mm)
First land part length	2.4 (mm)
Last land part length	2.4 (mm)
Groove seal total length	35.2 (mm)
Number of groove	10
Clearance of groove seal (C_r)	0.175 (mm)
Radius of groove seal	35.2 (mm)
Normalized inlet-tangential velocity	0.1
Inlet loss coefficient (ξ_{in})	0.05
Pressure recovery factor (ξ_{ex})	0.95
Loss coefficient (ξ_{12})	0.05
Rotor speed	500 (RPM)
Density	998.2 (Kg/m³)
Absolute viscosity	0.001 (N-s/m²)
Groove penetration angle (α)	0.008 (radian)
(n_s, m_s) for stator surface	0.079, −0.25
(n_r, m_r) for rotor surface	0.079, −0.25

Fig. 6   Direct stiffness coefficient vs. rotor speed

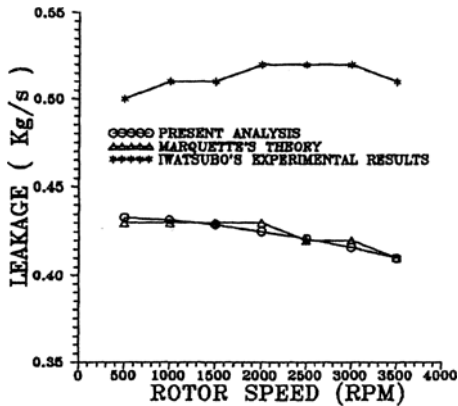**Fig. 7**   Cross coupled stiffness coefficient vs. rotor speed

Fig. 5   Leakage vs. rotor speed

and Marquette and Childs' are both about 17% less than Iwatsubo and Sheng's experimental values. The analytical results both show that the leakage is decreasing as the rotor speed is increased but the experimental result shows the opposite trend.

Figure 6 illustrates the result for the direct stiffness coefficient (K) vs. rotor speed. The direct stiffness is found to be related with the critical
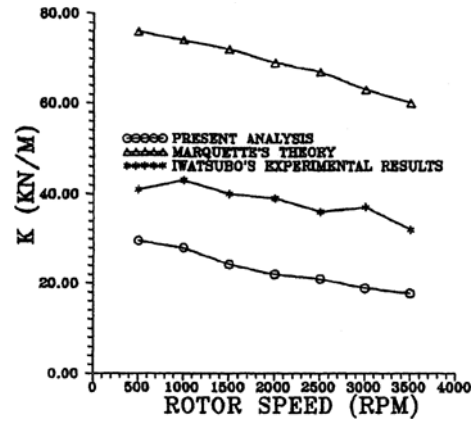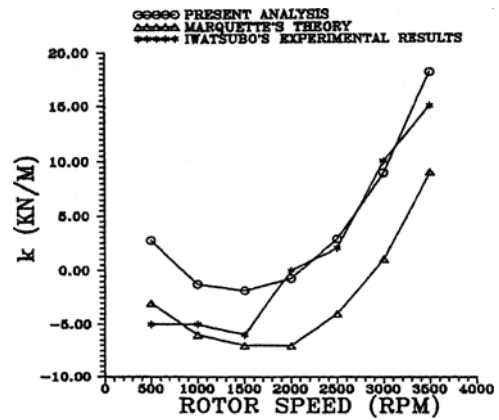
speed. The present analysis provides improved estimation of the direct stiffness compared with Marquette and Childs' theoretical result. The present analysis underpredicts the direct stiffness compared with Iwatsubo and Sheng's experimental result, while Marquette and Childs' analysis overpredicts. Generally, the direct stiffness is shown to be decreasing as the rotor speed is increased.

The cross-coupled stiffness coefficient represents the tangential component of the seal's rotor-dynamic force acting on the rotor which is precessing in the direction of the rotation. A positive cross-coupled stiffness that increases the forward precessing motion has a destabilizing effect. Figure 7 shows that the present analysis predicts the cross-coupled stiffness to be higher than the
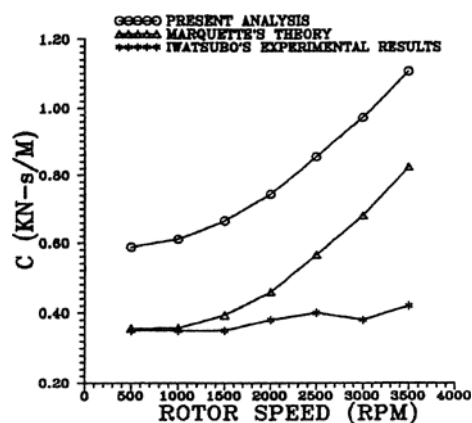
Fig. 8 Direct damping coefficient vs. rotor speed

Table 2 Comparisons between circumferentially grooved seal and smooth seal

	$\dot{Q}$ (Kg/s)	K (KN/m)	k (KN/m)	C(KN-s/m)	$k/(\omega C)$
Grooved seal	0.433	29.6	2.7	0.59	0.088
Smooth seal	0.608	1255	36.1	5.3	0.12

predicted value of Marquette and Childs' theoretical analysis and is in fact a much better fit to Iwatsubo and Sheng's experimental result for the range of over 2,000 rpm. As the rotor speed is increasing in the range of over 1500 rpm, the cross-coupled stiffness coefficient is rapidly increases.

The direct damping coefficient represents the tangential component of the seal's rotordynamic force opposing the precessional motion and has a stabilizing effect. The present analysis predicts the direct damping coefficient to be higher than Marquette and Childs' theoretical analysis and Iwatsubo and Sheng's experimental results as shown in Fig. 8. The present analysis provides worse prediction than that of Marquette and Childs' theoretical analysis. The present analysis shows that the direct damping coefficient rapidly increases as the rotor speed is increased, but the experimental sesult indicates the direct damping coefficent to stay almost constant.

As shown in Figs. 5~8, even though the present analysis partially improves on Marquette and Childs' theoretical analysis there is still room for further improvement. The assumption of single-vortex flow within the groove cavity and the interface jet shear stress definition used in present three-control-volume analysis may not adequately represent a rather complicated flow existing in the groove cavity. A more sophisticated model for describing the actual groove cavity flow and many more experimental results are needed to further improve on the theoretical analysis.

Table 2 provides the theoretical comparisons of the leakage and rotordynamic coefficients between the circumferentially grooved and the smooth annular seals (Ha (1998)). In the comparisons, the dimensions and operating conditions of the smooth seal are the same as the grooved seal case (see Fig. 1 and Table 1). As shown in Table 2, the grooved seal can reduce the leakage by about 30% compared to the smooth seal to yield a corresponding increase in the pump efficiency. The direct stiffness and cross-coupled stiffness of the grooved seal are much smaller than those of the smooth seal case. The whirl frequency ratio $(k/\omega C)$ is a ratio of the destabilizing forces to the stabilizing forces and should be minimized from the rotordynamic point of view. The whirl frequency ratio of the grooved seal shows a smaller value than that of the smooth seal case. Consequently, the grooved seal can be used as wear-ring, inter-stage, and balance piston seals in pumps instead of the smooth seal for improved leakage control and rotordynamic characteristics.

5. Conclusions

The leakage prediction and rotordynamic analysis of an annular seal with smooth rotor and circumferentially grooved stator are developed based on a three-control-volume theory. The present analysis is validated by comparing with previously problished experimental and theoretical results. The results of the present analysis support the following conclusions.

(1) For the leakage prediction, the present analysis shows a good agreement with Marquette and Childs' theoretical result, but underpredicts by 17% compared to Iwatsubo and Sheng's

experimental result.

(2) For the direct stiffness coefficient, the present analysis predicts a lower value than Marquette and Childs' theoretical result as well as Iwatsubo and Sheng's experimental result, but yields a better prediction than Marquette and Childs' theoretical analysis.

(3) For the cross-coupled stiffness coefficient, the present analysis shows a good agreement with Iwatsubo and Sheng's experimental result for the range of over 2,000 rpm.

(4) For the direct damping coefficient, the present analysis yields a higher value than Marquette and Childs' theoretical result and shows a poor agreement with Iwatsubo and Sheng's experimental result.

(5) In the theoretical comparisons of the leakage and rotordynamic coefficients between the circumferentially grooved and smooth annular seals with the identical dimensions and operating conditions, the grooved seal shows better leakage and stability characteristics from the rotordynamic point of view.

References

Black, H. F., and Cochran, E. A., 1973, "Leakage and Hybrid Bearing Properties of Serrated Seals in Centrifugal Pumps," *presented at the 6th International Conference on Fluid Sealing*, Munich, Germany, G5-61-G5-70.

Childs, D. W., and Kim, C. H., 1986, "Testing for Rotordynamic Coefficients and Leakage : Circumferentially-Grooved Turbulent Annular Seals," *in Proceedings of the Second IFToMM International Conference on Rotordynamics*, Tokyo, Japan, pp. 609—618.

Florjancic, S., 1990, "Annular Seals of High Energy Centrifugal Pumps : A New Theory and Full Scale Measurement of Rotordynamic Coefficients and Hydraulic Friction Factors," Ph. D. Dissertation, Swiss Federal Institute of Technology, Zurich, Switzerland.

Ha, T. W., 1998, "Hydrodynamic Forces of Impeller Shroud and Wear-ring Seal on Centrifugal Pump," *KSME Journal* Vol. A, No. 22, pp. 102—110.

Hirs, G., 1973, "A Bulk-Flow Theory for Turbulence in Lubrication Films," *ASME Journal of Lubrication Technology*, pp. 137—146.

Iwatsubo, T., and Sheng, B., 1990, "Evaluation of Dynamic Characteristics of Parallel Grooved Seals by Theory and Experiment," *in Proceedings of the Third IFToMM International Conference on Rotordynamics*, Lyon, France, pp. 313—318.

Iwatsubo, T., Sheng, B., and Ono, M., 1990, "Experiment of Static and Dynamic Characteristics of Spiral Grooved Seals," *Rotordynamic Instability Problems in High-Performance Turbomachinery*, NASA CP No. 3122, Proceedings of a workshop held at Texas A&M University, pp. 223—234.

Kilgore, J. J., and Childs, D. W., 1990, "Rotordynamic Coefficients and Leakage Flow of Circumferentially Grooved Liquid-Seals," *ASME Journal of Fluids Engineering*, Vol. 112, pp. 250—256.

Kim, C. H., and Childs, D. W., 1987, "Analysis for Rotordynamic Coefficients of Helically-Grooved Turbulent Annular Seals," *ASME Journal of Tribology*, Vol. 109(1), pp. 136—143.

Marquette, O. R., and Childs D. W., 1996, "An Extended Three-Control-Volume Theory for Circumferentially-Grooved Liquid Seals," *ASME Journal of Tribology*, Vol. 118, pp. 276—285.

Meirovitch, L., 1985, *Introduction to Dynamics and Control*, Wiley Interscience, New York.

Nordmann, R., Dietzen, F. J., Janson, W., Frei, A., and Florjancic, S., 1986, "Rotordynamic Coefficients and Leakage Flow of Parallel Grooved Seals and Smooth Seals," *Rotordynamic Instability Problems in High-Performance Turbomachinery*, NASA CP No. 2338, Proceedings of a workshop held at Texas A&M University, pp. 129—153.

Wyssman, H., Pham, T., and Jenny, R., 1984, "Prediction of Stiffness and Damping Coefficients for Centrifugal Compressor Labyrinth Seals," *ASME Journal of Engineering for Gas Turbines and Power*, Vol. 106, pp. 920—926.

Appendix A

A.1 Nondimensional Governing Equations

A.1.1 Control volume I

$$\frac{\partial}{\partial \tau}(h_I) + \frac{\partial}{\partial \theta}(h_I u_I) + \frac{1}{T\omega}\frac{\partial}{\partial z}(h_I w_I) = 0$$

$$-h_I \frac{\partial p_I}{\partial z} = \frac{L}{C_r}\left[\frac{n_s}{2}R_{sI}{}^{ms}w_I{}^2\right.$$

$$\left(1 + b^2\left(\frac{u_I}{w_I}\right)^2\right)^{\frac{ms+1}{2}}\right] + \frac{L}{C_r}\left[\frac{n_r}{2}R_{sI}{}^{mr}w_I{}^2\right.$$

$$\left(1 + b^2\left(\frac{(u_I-1)}{w_I}\right)^2\right)^{\frac{mr+1}{2}}\right]$$

$$+ h_I\left[(T\omega)\frac{\partial w_I}{\partial \tau} + w_I\frac{\partial w_I}{\partial z} + (T\omega)u_I\frac{\partial w_I}{\partial \theta}\right]$$

$$-h_I\frac{\partial p_I}{\partial \theta} = \frac{bR}{C_r}\left[\frac{n_s}{2}R_{sI}{}^{ms}w_I u_I\right.$$

$$\left(1 + b^2\left(\frac{u_I}{w_I}\right)^2\right)^{\frac{ms+1}{2}}\right]$$

$$+ \frac{bR}{C_r}\left[\frac{n_r}{2}R_{sI}{}^{mr}w_I(u_I-1)\right.$$

$$\left(1 + b^2\left(\frac{u_I-1}{w_I}\right)^2\right)^{\frac{mr+1}{2}}\right]$$

$$+ b^2 h_I\left[\frac{\partial u_I}{\partial \tau} + \frac{1}{T\omega}w_I\frac{\partial u_I}{\partial z} + u_I\frac{\partial u_I}{\partial \theta}\right]$$

$$R_{sI} = \frac{2H_I W_I}{\nu}$$

A.1.2 Control volume II

$$\frac{\partial}{\partial \tau}(h_{II}) + \frac{\partial}{\partial \theta}(h_{II}u_{II}) + \frac{1}{T\omega}\frac{\partial}{\partial z}(h_{II}w_{II})$$

$$+ \frac{B}{C_r}h_{III}\frac{\partial}{\partial \theta}(u_{III}) = 0$$

$$-h_{II}\frac{\partial p_{II}}{\partial z} = \frac{L}{C_r}\left[\frac{n_r}{2}R_{sII}{}^{mr}w_{II}{}^2\right.$$

$$\left(1 + b^2\left(\frac{u_{II}-1}{w_{II}}\right)^2\right)^{\frac{mr+1}{2}}\right] + \frac{L}{C_r}[1.88\beta_z{}^2|v_{II}$$

$$- v_{III}|(w_{II} - \bar{w}_{III})] + h_{II}\left[(T\omega)\frac{\partial w_{II}}{\partial \tau}\right.$$

$$+ w_{II}\frac{\partial w_{II}}{\partial z} + (T\omega)u_{II}\frac{\partial w_{II}}{\partial \theta}\right]$$

$$+ \frac{LB\omega}{C_r W_o}h_{III}\frac{\partial u_{III}}{\partial \theta}(w_j - w_{II})$$

$$-h_{II}\frac{\partial p_{II}}{\partial \theta} = \frac{bR}{C_r}\left[\frac{n_r}{2}R_{sII}{}^{mr}w_{II}(u_{II}-1)\left(1\right.\right.$$

$$\left.+ b^2\left(\frac{u_{II}-1}{w_{II}}\right)^2\right)^{\frac{mr+1}{2}}\right] + \frac{bR}{C_r}[1.88\beta_\theta{}^2|v_{II} - v_{III}|$$

$$(u_{II} - u_{III})] + b^2 h_{II}\left[\frac{\partial u_{II}}{\partial \tau} + \frac{1}{T\omega}w_{II}\frac{\partial u_{II}}{\partial z}\right.$$

$$\left. + u_{II}\frac{\partial u_{II}}{\partial \theta}\right] + \frac{b^2 B}{C_r}h_{III}\frac{\partial u_{III}}{\partial \theta}(u_j - u_{II})$$

$$R_{sII} = \frac{2H_{II}W_{II}}{\nu}$$

A.1.3 Control volume III

$$B\omega h_{III}\frac{\partial u_{III}}{\partial \theta} - W_o V = 0$$

$$-h_{III}\frac{\partial p_{II}}{\partial \theta} = \frac{bR}{B}\left[\frac{n_s}{2}R_{sIII}{}^{ms}\bar{w}_{III}u_{III}\left(1\right.\right.$$

$$\left.+ b^2\left(\frac{u_{III}}{\bar{w}_{III}}\right)^2\right)^{\frac{ms+1}{2}}\right] - \frac{bR}{B}[1.88\beta_\theta{}^2|v_{II} - v_{III}|$$

$$(u_{II} - u_{III})] - \frac{bR}{L}\frac{\partial}{\partial z}(h_{III}\tau_{gw\theta})$$

$$+ b^2 h_{III}\left[\frac{\partial u_{III}}{\partial \tau} + u_{III}\frac{\partial u_{III}}{\partial \theta}\right] + b^2 h_{III}\frac{\partial u_{III}}{\partial \theta}$$

$$(u_{III} - u_j)$$

$$\tau_{gw\theta}(z) = \tau_{gw\theta}(0) + \left[\frac{\tau_{gw\theta}(L_g) - \tau_{gw\theta}(0)}{L_g}\right]z$$

$$R_{sIII} = \frac{2H_{III}\bar{W}_{III}}{\nu}$$

Appendix B

B.1 Zeroth-order Governing Equations

B.1.1 Control volume I

$$h_0 w_{I0} = 1$$

$$\frac{\partial p_{I0}}{\partial z} = -\frac{1}{h_{I0}}\frac{L}{C_r}\left[\frac{n_s}{2}R_{sI0}{}^{ms}w_{I0}{}^2\left(1 + b^2\right.\right.$$

$$\left.\left(\frac{u_{I0}}{w_{I0}}\right)^2\right)^{\frac{ms+1}{2}}\right] - \frac{1}{h_{I0}}\frac{L}{C_r}\left[\frac{n_r}{2}R_{sI0}{}^{mr}w_{I0}{}^2\right.$$

$$\left(1 + b^2\left(\frac{(u_{I0}-1)}{w_{I0}}\right)^2\right)^{\frac{mr+1}{2}}\right]$$

$$\frac{\partial u_{I0}}{\partial z} = -\frac{1}{h_{I0}}\frac{L}{C_r}\left[\frac{n_s}{2}R_{sI0}{}^{ms}u_{I0}\right.$$

$$\left(1 + b^2\left(\frac{u_{I0}}{w_{I0}}\right)^2\right)^{\frac{ms+1}{2}}\right] - \frac{1}{h_{I0}}\frac{L}{C_r}\left[\frac{n_r}{2}R_{sI0}{}^{mr}\right.$$

$$(u_{I0}-1)\left(1 + b^2\left(\frac{(u_{I0}-1)}{w_{I0}}\right)^2\right)^{\frac{mr+1}{2}}\right]$$

$$R_{sI0} = \frac{2C_r h_{I0} W_o w_{I0}}{\nu}$$

B.1.2 Control volume II

$$h_{II0} w_{II0} = 1$$

$$\frac{\partial p_{II0}}{\partial z} = -\frac{L}{C_r}\frac{1}{h_{II0}}\left[\frac{1}{2}f_{rII0}u_{rII0}w_{II0}\right.$$

$$\left.+ 1.88\beta_z{}^2|v_{II0} - v_{III0}|(w_{II0} - \bar{w}_{III0})\right]$$

$$+ \frac{1}{h_{II0}{}^3}\frac{\partial h_{II0}}{\partial z}$$

$$\frac{\partial u_{II0}}{\partial z} = -\frac{L}{C_r}\left[\frac{1}{2}f_{rII0}u_{rII0}(u_{II0}-1)\right.$$
$$\left. + 1.88\beta_\theta^2|v_{II0}-v_{III0}|(u_{II0}-u_{III0})\right]$$

$$u_{rII0} = (w_{II0}^2 + b^2(u_{II0}-1)^2)^{\frac{1}{2}}$$
$$f_{rII0} = n_r(Re_a h_{II0} u_{rII0})^{m_r}$$
$$Re_a = \frac{2C_r W_0}{\nu}$$
$$|V_{II0} - V_{III0}|^2 = b^2(U_{II0} - U_{III0})^2 + (W_{II0} - \bar{W}_{III})^2$$
$$h_{II0}(z) = 1 + \frac{L}{C_r}z\tan\alpha$$

B.1.3 Control volume III

$$0 = \frac{bR}{B}\left[\frac{1}{2}f_{sIII0}u_{sIII0}u_{III0} - 1.88\beta_\theta^2|v_{II0}\right.$$
$$\left. - v_{III0}|(u_{II0}-u_{III0})\right] + \frac{bR}{2L}h_{III0}$$
$$(f_{sIII0}u_{sIII0}u_{III0}|_0 + f_{sIII0}u_{sIII0}u_{III0}|_1)$$
$$+ \frac{bR}{2L}\frac{\partial h_{III0}}{\partial z}(f_{sIII0}u_{sIII0}u_{III0}|_0(z-1)$$
$$+ f_{sIII0}u_{sIII0}u_{III0}|_1 z)$$

$$u_{sIII0} = (\bar{w}_{III}^2 + b^2 u_{III0}^2)^{\frac{1}{2}}$$
$$f_{sIII0} = n_s(Re_c h_{III0} u_{sIII0})^{m_s}$$
$$Re_c = \frac{2BW_0}{\nu}$$

$$h_{III0}(z) = 1 - \frac{L}{B}z\tan\alpha$$

B.2 First-order Governing Equations

B.2.1 Control volume I

$$\frac{\partial w_{I1}}{\partial z} + \omega T\frac{\partial u_{I1}}{\partial \theta} + \frac{w_{I1}}{h_{I0}}\frac{dh_{I0}}{dz}$$
$$= -\frac{1}{h_{I0}}\left(w_{I0}\frac{\partial h_{I1}}{\partial z} + (T\omega)u_{I0}\frac{\partial h_{I1}}{\partial \theta}\right.$$
$$\left. + (T\omega)\frac{\partial h_{I1}}{\partial \tau}\right) + \frac{h_{I1}w_{I0}}{h_{I0}^2}\frac{\partial h_{I0}}{\partial z}$$

$$\frac{\partial p_{I1}}{\partial z} + \left[\frac{(\sigma_{sI0}(m_s+1)\beta_1 + \sigma_{rI0}(m_r+1)\beta_0)w_{I0}}{2h_{I0}}\right]u_{I1}$$
$$+ \left[\frac{d(w_{I0})}{dz} + \left(\frac{((2+m_r)\sigma_{rI0} + (2+m_s)\sigma_{sI0})w_{I0}}{2h_{I0}}\right)\right]w_{I1}$$
$$- \left[\frac{((1+m_s)\sigma_{sI0}\beta_1 u_{I0} + (1+m_r)\sigma_{rI0}\beta_0(u_{I0}-1))}{2h_{I0}}\right]w_{I1}$$
$$+ \left[(\omega T)\frac{\partial w_{I1}}{\partial \tau} + (\omega T)u_{I0}\frac{\partial w_{I1}}{\partial \theta} + w_{I0}\frac{\partial w_{I1}}{\partial z}\right]$$
$$= h_{I1}\left[\frac{w_{I0}^2}{2h_{I0}^2}(\sigma_{sI0}(1-m_s) + \sigma_{rI0}(1-m_r))\right]$$

$$\frac{L}{bR}\frac{\partial p_{I1}}{\partial \theta} + \left[(\omega T)\frac{\partial u_{I1}}{\partial \tau} + (\omega T)u_{I0}\frac{\partial u_{I1}}{\partial \theta}\right.$$

$$+ w_{I0}\frac{\partial u_{I1}}{\partial z}\right] + \frac{1}{2h_{I0}}[w_{I0}(\sigma_{rI0}+\sigma_{sI0}) + \sigma_{rI0}$$
$$(m_r+1)(u_{I0}-1)\beta_0 + \sigma_{sI0}(m_s+1)u_{I0}\beta_1]u_{I1}$$
$$+ \frac{1}{2h_{I0}}[\sigma_{rI0}(u_{I0}-1)[m_r - (1+m_r)\beta_0(u_{I0}$$
$$-1)/w_{I0}]]w_{I1} + \frac{1}{2h_{I0}}[\sigma_{sI0}u_{I0}[m_s - (1+m_s)$$
$$\beta_1 u_{I0}/w_{I0}]]w_{I1} = \frac{h_{I1}}{2h_{I0}}[w_{I0}[(1-m_r)(u_{I0}$$
$$-1)\sigma_{rI0} + (1-m_s)u_{I0}\sigma_{sI0}]/h_{I0}]$$

$$\sigma_{sI0} = \frac{L}{C_r}n_s R_{sI0}{}^{m_s}\left[1 + b^2\left(\frac{u_{I0}}{w_{I0}}\right)^2\right]^{\frac{m_s+1}{2}}$$
$$\sigma_{rI0} = \frac{L}{C_r}n_r R_{sI0}{}^{m_r}\left[1 + b^2\left(\frac{u_{I0}-1}{w_{I0}}\right)^2\right]^{\frac{m_r+1}{2}}$$
$$\beta_0 = \frac{b^2(u_{I0}-1)}{w_{I0}[1 + b[(u_{I0}-1)/w_{I0}]^2}$$
$$\beta_1 = \frac{b^2 u_{I0}}{w_{I0}}[1 + [bu_{I0}/w_{I0}]^2$$

B.2.2 Control volume II

$$L_1\frac{\partial h_{II1}}{\partial \tau} + L_2\frac{\partial h_{II1}}{\partial \theta} + L_3\frac{\partial h_{II1}}{\partial z} + L_4\frac{\partial u_{II1}}{\partial \theta}$$
$$+ L_5\frac{\partial u_{III1}}{\partial \theta} + L_6\frac{\partial w_{III1}}{\partial z} + L_7 h_{II1} + L_8 w_{III1} = 0$$

$$M_1\frac{\partial p_{II1}}{\partial z} + M_2 h_{II1} + M_3\frac{\partial w_{III1}}{\partial \tau} + M_4\frac{\partial w_{III1}}{\partial \theta}$$
$$+ M_5\frac{\partial w_{III1}}{\partial z} + M_6\frac{\partial u_{III1}}{\partial \theta} + M_7 u_{II1} + M_8 u_{III1}$$
$$+ M_9 w_{III1} = 0$$

$$N_1\frac{\partial p_{II1}}{\partial \theta} + N_2\frac{\partial u_{II1}}{\partial \tau} + N_3\frac{\partial u_{II1}}{\partial \theta} + N_4\frac{\partial u_{II1}}{\partial z}$$
$$+ N_5\frac{\partial u_{III1}}{\partial \theta} + N_6 h_{II1} + N_7 u_{II1} + N_8 u_{III1}$$
$$+ N_9 w_{III1} = 0$$

$$L_1 = \frac{bL}{R}, \quad L_2 = \frac{bL}{R}u_{II0}, \quad L_3 = w_{II0},$$
$$L_4 = \frac{bL}{R}h_{II0}, \quad L_5 = \frac{bBL}{C_r R}h_{III0}, \quad L_6 = h_{II0},$$
$$L_7 = \frac{\partial w_{II0}}{\partial z}, \quad L_8 = \frac{\partial h_{II0}}{\partial z}$$

$$M_1 = 1, \quad M_2 = -\frac{1}{h_{II0}}\frac{\partial p_{II0}}{\partial z} + \frac{L}{2C_r}$$
$$\frac{w_{II0}}{h_{II0}^2}u_{rII0}f_{rII0}m_r + \frac{bL}{R}\frac{w_{II0}}{h_{II0}}\frac{\partial w_{II0}}{\partial z}$$
$$M_3 = \frac{bL}{R}, \quad M_4 = \frac{bL}{R}u_{II0}, \quad M_5 = \frac{bL}{R}w_{II0},$$
$$M_6 = \frac{bBL}{RC_r}\frac{h_{III0}}{h_{II0}}(w_{j0} - w_{II0}),$$
$$M_7 = \frac{L}{C_r}\frac{1}{h_{II0}}\left(\frac{1}{2}f_{II0}w_{II0}b^2(1+m_r)\frac{u_{II0}-1}{u_{rII0}}\right.$$

$$+1.88\beta_z^2 b^2 \frac{u_{II0}-u_{III0}}{|v_{II0}-v_{III0}|}(w_{II0}-\bar{w}_{III}))$$

$$M_8 = -\frac{L}{C_r}\frac{1}{h_{II0}}1.88\beta_z^2 b^2 \frac{u_{II0}-u_{III0}}{|v_{II0}-v_{III0}|}(w_{II0}-\bar{w}_{III})$$

$$M_9 = \frac{bL}{R}\frac{\partial w_{II0}}{\partial z} + \frac{L}{C_r}\frac{1}{h_{II0}}\Big(f_{rII0}u_{rII0}$$

$$+\frac{1}{2}m_r f_{rII0}u_{rII0} - \frac{1}{2}f_{rII0}b^2(1+m_r)$$

$$\frac{(u_{II0}-1)^2}{u_{rII0}} + 1.88\beta_z^2\Big[|v_{II0}-v_{III0}|$$

$$+\frac{(w_{II0}-\bar{w}_{III})^2}{|v_{II0}-v_{III0}|}\Big]\Big)$$

$$N_1 = 1, \quad N_2 = b^2, \quad N_3 = b^2 u_{II0}, \quad N_4 = \frac{bL}{R}w_{II0},$$

$$N_5 = \frac{b^2 B}{C_r}\frac{h_{III0}}{h_{II0}}(u_{j0}-u_{II0}),$$

$$N_6 = \frac{bL}{R}\frac{w_{II0}}{h_{II0}}\frac{\partial u_{II0}}{\partial z} + \frac{bC_r}{R}\frac{1}{h_{II0}^2}$$
$$\frac{1}{2}f_{II0}m_r u_{rII0}(u_{II0}-1)$$

$$N_7 = \frac{bR}{C_r}\frac{1}{h_{II0}}\Big(\frac{1}{2}f_{rII0}u_{rII0} + \frac{1}{2}f_{rII0}b^2(1$$

$$+m_r)\frac{(u_{II0}-1)^2}{u_{rII0}} + 1.88\beta_\theta^2$$

$$\frac{b^2(u_{II0}-u_{III0})^2+|v_{II0}-v_{III0}|^2}{|v_{II0}-v_{III0}|}\Big)$$

$$N_8 = -\frac{bR}{C_r}\frac{1}{h_{II0}}1.88\beta_\theta^2$$

$$\frac{b^2(u_{II0}-u_{III0})^2+|v_{II0}-v_{III0}|^2}{|v_{II0}-v_{III0}|}$$

$$N_9 = \frac{bR}{L}\frac{\partial u_{II0}}{\partial z} + \frac{bR}{C_r}\frac{1}{h_{II0}}\Big(\frac{1}{2}(1+m_r)$$

$$f_{rII0}u_{rII0}\frac{(u_{II0}-1)}{w_{II0}} - \frac{1}{2}f_{rII0}b^2(1+m_r)$$

$$\frac{(u_{II0}-1)^3}{u_{rII0}w_{II0}} + 1.88\beta_\theta^2\frac{u_{II0}-u_{III0}}{|v_{II0}-v_{III0}|}(w_{II0}$$

$$-\bar{w}_{III}))$$

B.2.3 Control volume Ⅲ

$$O_1\frac{\partial p_{III}}{\partial\theta} + O_2\frac{\partial u_{III}}{\partial\tau} + O_3\frac{\partial u_{III}}{\partial\theta} + O_4 u_{III}$$

$$+O_5 u_{III} + O_6 w_{III} = 0$$

$$O_1 = 1, \quad O_2 = b^2, \quad O_3 = b^2(2u_{III0}-u_{j0}),$$

$$O_4 = -\frac{bR}{B}\frac{1}{h_{III0}}1.88\beta_\theta^2\frac{u_{II0}-u_{III0}}{|v_{II0}-v_{III0}|}(w_{II0}$$

$$-\bar{w}_{III}),$$

$$O_5 = \frac{bR}{B}\frac{1}{h_{III0}}\Big(\frac{1}{2}f_{sIII0}u_{sIII0} + \frac{1}{2}f_{sIII0}(1$$

$$+m_s)b^2\frac{u_{III0}^2}{u_{sIII0}} + 1.88\beta_\theta^2\frac{u_{II0}-u_{III0}}{|v_{II0}-v_{III0}|}(w_{II0}$$

$$-\bar{w}_{III})\Big)$$

$$O_6 = -\frac{bR}{B}1.88\beta_\theta^2\frac{(u_{II0}-u_{III0})}{|v_{II0}-v_{III0}|}(w_{II0}-\bar{w}_{III})$$